



## Synergistic Action and Enhanced Therapeutic Properties of rGO-ZnO Nanocomposites using *Ixora coccinea* and *Prosopis juliflora*

Ammu Chandhini Arivoli<sup>1</sup>, Preethy Kuppusamy Ravichandran<sup>2</sup>, Meenakshi Sivalingam Valliappan<sup>3</sup>, Sivakumar Kandhasamy\*

<sup>1</sup>Department of Biomedical Engineering, Karpaga Vinayaga College of Engineering and Technology, Chengalpattu, Tamil Nadu, India- 603308

<sup>2</sup>Department of Biotechnology, St. Joseph's College of Engineering, Chennai, 600119 Tamil Nadu, India

<sup>3</sup>Department of Biotechnology, Karpaga Vinayaga College of Engineering and Technology, Chengalpattu, 603308 Tamil Nadu, India-

<sup>4</sup>Department of Biomedical Engineering & Department of Biotechnology, Karpaga Vinayaga College of Engineering and Technology, Chengalpattu, 603308 Tamil Nadu, India

\*Corresponding Author's Email: [ksivakumar76@gmail.com](mailto:ksivakumar76@gmail.com)

### Abstract

The present study focuses on the green synthesis of zinc oxide (ZnO) nanoparticles and reduced graphene oxide–zinc oxide (rGO–ZnO) nanocomposites using the phytoextract from the flowers of *Ixora coccinea* as a non-toxic reducing agent and stabilizer. The main hypothesis in this investigation is that the bioactive phytochemicals contained in *I. coccinea* flowers can enhance the physicochemical and biological properties of ZnO nanoparticles with less harmful chemical alternatives. Furthermore, cellulose extracted from agricultural biomass (*Setaria italica*) was used to synthesize graphene oxide as a form of sustainability. The synthesized nanocomposites were made using a simple magnetic stirring approach and were characterized with UV–Vis, XRD, FTIR, SEM, and EDS analysis, indicating euchoite crystallized structure with uniform ZnO loading on the surface of rGO. The rGO–ZnO nanocomposite displayed strong antioxidant, antibacterial, antibiofilm, antidiabetic, and anti-inflammatory properties, while showing significant hemocompatibility (0.5% hemolysis). These findings offer improved therapeutic activity when compared with the base ZnO solution. This research illustrates a viable route for the green synthesis of multifunctional nanocomposites with potential applications in biomedical, pharmaceutical, and environmental science, while highlighting the possible synergistic action of green-synthesized rGO–ZnO nanostructured materials.

**Keywords:** Antibacterial Activity, Biofilm; Graphene Oxide; Nanocomposite

### Introduction

This research looks at rGO-ZnO nanocomposites exhibiting combined and improved therapeutic actions constructed from plant extracts from *Ixora coccinea* and *Prosopis juliflora*. Plant extracts provide a greener option to chemically reducing graphene oxide and take advantage of plant-derived reducing and stabilizing mechanisms in some phytochemical biosynthetic agents (Abdelfatah *et al.*, 2022). Green synthesis is environmentally friendly with inherently low toxicities and results in biocompatibility and multifunctionality of the resultant nanocomposites (Dar *et al.*, 2021). The sharp edges of a layer of graphene oxide have the ability to physically penetrate and disrupt a bacterial cell membrane, exposing the cytoplasm to leaking, thus hindering nutrient uptake within the cell (Ilie *et al.*, 2022). Zinc oxide

nanoparticles, when incorporated into a nanocomposite, provide pathogen-killing properties through the production of reactive oxygen species and by liberating  $Zn^{2+}$  ions to compromise membrane integrity and other metabolism-related processes (Saravanan et al., 2023). Incorporating these actions of the rGO-ZnO composite synthesized from plant extracts containing bioactive compounds can demonstrate an augmented antimicrobial ability and actions of other biological functions such as antioxidant and anti-inflammatory actions (Sodeinde et al., 2022; Elbasuney et al., 2021). Ultimately, graphene composites demonstrated biocompatibility and possessed lower toxicities, which are important when investigating their use as agents of advanced biomedical research applications (Ilie et al., 2022; Hussein & Yassir, 2024).

Nanoparticles have high surface-to-volume ratios, which means that surface functionalization takes less work. This gives them amazing biological and catalytic properties (Majeed et al., 2019). Ostrovsky et al. (2009); Barui et al. (2018) have highlighted the low toxicity, biodegradability, and cost-effectiveness of zinc oxide nanoparticles, prompting their investigation for therapeutic and diagnostic applications. Zinc is an essential trace element in the body, playing a vital role in homeostasis, immunological responses, oxidative stress, apoptosis, aging, inhibiting free radical production, and restoring immune function (Stefanidou et al., 2006). Zinc oxide offers several applications in biomedicine, such as drug administration, antimicrobial properties, and wound dressings, hence challenging conventional therapies (Khorasani et al., 2018; Sruthi et al., 2018; Wiesmann et al., 2020). Multiple methods synthesize zinc oxide nanoparticles, but they are costly, labor-intensive, and pose safety risks (Yuvakkumar et al., 2014). Using plant extracts for green synthesis is a quick, cheap, and environmentally friendly alternative (Jadoun et al., 2021). This makes it suitable for biomedical uses (De Matteis et al., 2020), and it reduces the need for dangerous chemicals and high energy use (Kalpana & Rajeswari, 2018). *I. coccinea*, a plant known for its medicinal properties, to produce zinc oxide nanoparticles as a capping agent, and used zinc acetate dihydrate to speed up the reduction process (Baliga & Kurian, 2012). Phytochemicals in the extract, like carotenoids, phenolic acids, flavonoids, and sterols, work as reducing and stabilizing agents (Bandeira et al., 2020), making it easier for metal ions to reduce and stabilize in nanocomposites (Luque et al., 2018). Different forms of graphene, like Graphene Oxide (GO) and Reduced Graphene Oxide (rGO) (Durmus et al., 2019; Mandal et al., 2019), show great potential as nanomaterials for use in medicine (Yang et al., 2013; Campbell et al., 2019), and their excellent mechanical, electrical, and thermal properties (Garaj et al., 2010; Yu et al., 2016). Carbon-based materials such as activated carbon (Nasrollahzadeh et al., 2018) and carbon dots (Bozetine et al., 2016) can facilitate the support of ZnO nanoparticles. Researchers employ reduced graphene oxide sheets to inhibit aggregation and obstruct electron-hole pair recombination in zinc oxide (Pei & Cheng, 2012; Sun et al., 2015; Coroş et al., 2019; Chamundeeswari & Preethy, 2024).

Researchers are developing nanocomposites based on metal oxides and GO/rGO due to their superior characteristics and synergistic effects. An rGO-ZnO composite is crucial for improving performance while minimizing adverse effects (Ahamed et al., 2021). A straightforward magnetic stirring technique is employed for manufacture. ZnO nanoparticles made using green methods are attached to rGO sheets. GO sheets are made by reducing GO using an improved Hummer's method and a phytoextract from *P. juliflora*. Coordination interactions or ion exchange adsorb zinc ions from zinc acetate and hydroxyl ions onto reduced graphene oxide sheets. This creates a  $Zn(OH)_4^{2-}$  intermediate, which is then broken down by water to make ZnO nanoparticles on the surface of the rGO, which changes the charge on the surface (Landström et al., 2021; Li et al., 2012). Zinc ions stick to rGO sheets, creating ZnO nanoparticles and serving as starting points for metal-based cations (Tai et al., 2016; Sharma et al., 2020). *I. coccinea* is indeed a well-studied medicinal and ornamental plant known for its rich phytochemical profile. Several secondary metabolites and phytoextracts have been identified in different parts of the plant (leaves, flowers, roots, and stems), which justify its use in nanomaterial synthesis due to their reducing and stabilizing abilities (Dontha et al., 2015). This study sought to integrate ZnO and rGO into a composite to augment therapeutic efficacy and boost biocompatibility.

## Material and Methods

### Preparation of phytoextract using flowers of *Ixora coccinea*

The synthesis of zinc oxide nanoparticles involved the extraction of phytoactive compounds from *Ixora coccinea* flowers. The *I. coccinea* flowers were collected from Chengalpattu Garden in Tamil Nadu. The samples were rinsed with distilled water, extracted in a 1:10 ratio using deionized water, and heated at 50°C for 30 minutes. The extracted samples were filtered, and extract was preserved at 4°C for further study. The phytochemical analysis on carbohydrates, tannins, phenols, alkaloids, flavonoids, steroids, gums, mucilage, saponins, oils, and lipids was carried out (Banu & Cathrine, 2015).

### Green Synthesis of Zinc Oxide Nanoparticles

The eco-friendly zinc oxide nanoparticles were made by heating 0.5M of zinc acetate dihydrate to 60°C and then adding *I. coccinea* flower extract. Followed by incrementally added 2M NaOH while stirring to increase the alkalinity. The sample was allowed the precipitate to dry overnight, resulting in the production of white nanoparticles (Fig. 1).

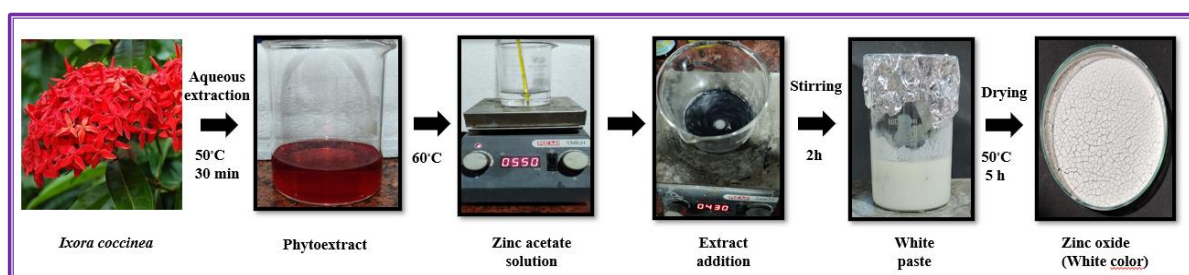


**Figure 1:** Scheme for the Synthesis of Zinc Oxide Nanoparticles from *I. Coccinea*

### Synthesis Of Graphene Oxide Using Enhanced Hummer's Method

*Setaria italica* bio-waste was carbonized in a controlled atmosphere at 800°C for 2 hours, and graphene oxide was produced utilizing the improved Hummer's process (Yadav & Lochab, 2019). The mixture of sulfuric acid and phosphoric acid in a 9:1 ratio with carbonaceous material and potassium permanganate in a 1:6 ratio oxidized it at 50°C for 8 hours, added deionized water in a 400:5 ratio, and introduced hydrogen peroxide to terminate the reaction. We rinsed the mixture with HCl, deionized water, and ethanol until it reached a neutral pH, then dried it to produce a brown-hued GO powder (Fig. 2).

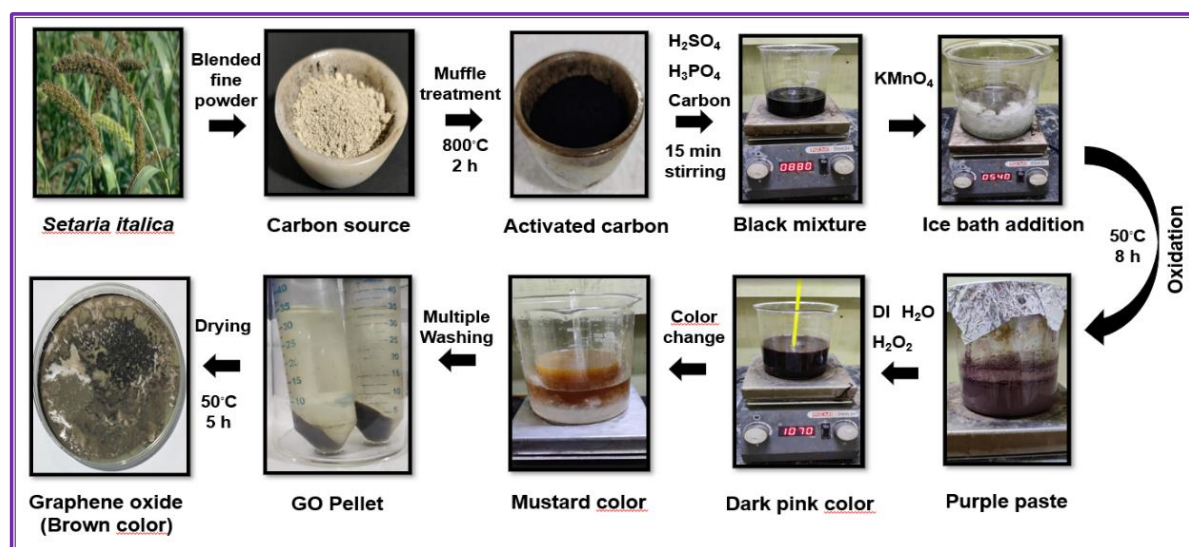


**Figure 2:** Scheme For Graphene Oxide Synthesis from *S. Italica* by Improved Hummer's Method

### Green Synthesis of Rgo

The sustainable synthesis of reduced graphene oxide (rGO) involved reducing GO using *P. juliflora* leaf extract, heating it at 121°C for 3 hours, and then washing and drying it to produce a black rGO powder (Haghighi & Tabrizi, 2013) (Fig. 3).

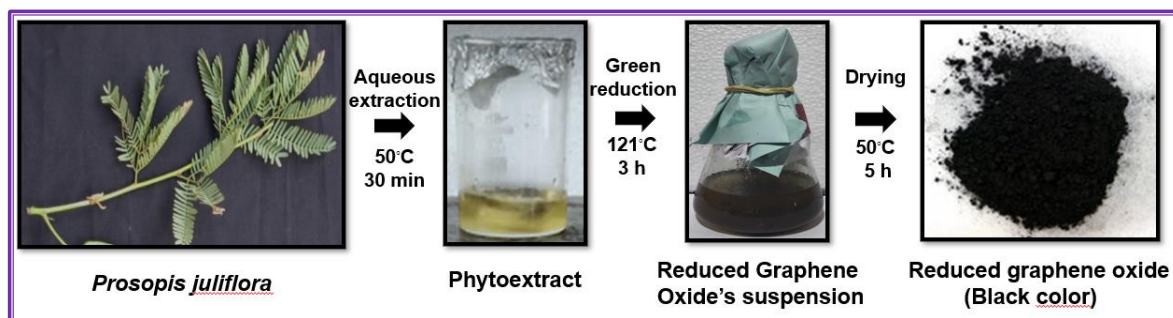


**Figure 3:** Scheme for Reduced Graphene Oxide Synthesis from *P. juliflora*

### Synthesis of Rgo - ZnO Composite by the Magnetic Stirring Method

The synthesized the rGO-ZnO composite using a magnetic stirring technique, coating the rGO and ZnO nanoparticles with equal amounts of water. We centrifuged and dehydrated the sample to produce a gray-hued composite. The loading rate was 8 mg/ml, signifying an adequate ZnO incorporation on rGO.

### Characterization Studies

The characterization of samples was carried out using XRD-7000, FT-IR, and A2060 systronic UV-Vis spectroscopy. The structural morphology was carried out using Carl Zeiss 6027 EDX and FE-SEM, and assessed the particle size distribution with Zeta sizer version 7.12. The amount of samples utilized for the subsequent experiments ranged from 100 to 1000 µg/ml, with increments of 200 µg/ml, and the activity was assessed.

### Antioxidant Activity

We used the DPPH assay to assess the synthesized ZnO and rGO-ZnO composite's ability to scavenge free radicals. The samples were added to the DPPH solution, incubated at 37°C for 30 minutes in darkness, and then measured and computed for their absorbance at 517 nm (Burits & Bucar, 2000).

### Anti-inflammatory Activity

The anti-inflammatory procedure involved the incorporation of 0.2 ml of egg albumin and 2.8 ml of phosphate-buffered saline into the samples, which were then vortexed. We incubated the solution at 37°C for 15 minutes, then at 70°C for 5 minutes, and measured the absorbance at 660 nm. Aceclofenac was used as a reference drug, and the anti-inflammatory effect was calculated (Dey et al., 2011).

### Antidiabetic Assay

The research assessed the anti-diabetic efficacy of live model yeast at glucose concentrations of 5 mM, 10 mM, and 25 mM, using metformin as the reference medication. We introduced samples to 1 ml of the prepared glucose solution and incubated them at 37°C for 10 minutes. Then 100 µl of yeast was added, and the mixture was left to sit at 37°C for an hour. The absorbance at 540 nm was then measured (Pitchaipillai & Ponniah, 2016).

### Biofilm Inhibition Assay

The assay for biofilm inhibition involved the incorporation of ZnO and rGO-ZnO composite samples into *E. coli* and incubated at 37°C for 48 hours, and rinsed it thrice with phosphate buffer, stained it with 0.5% crystal violet, washed it twice, and treated it with an ethanol-acetone mixture before measuring the absorbance at OD 595. The study also examined *B. subtilis* under similar conditions, and the percentage of biofilm inhibition was calculated (Lin et al., 2018; Sharma et al., 2015).

### Antibacterial Assay

The antibacterial assay utilized *B. subtilis* and *E. coli* inoculated into nutritional broth and incubated it at 37°C for 48 hours. We subsequently inoculated the cultures onto Petri dishes containing nutrient agar and perforated them. We introduced samples of ZnO and rGO-ZnO composites in volumes ranging from 20 to 100 µl and incubated them for 24 hours, using ampicillin as a control. The zone of inhibition assessed the antibacterial efficacy of the samples (Balouiri et al., 2016).

### Anticoagulation Assay

The anti-coagulation activity was evaluated using standard methods, with a negative control of a drop of blood with 1.6 mg/ml EDTA. Samples were added to 1 ml of blood and clotting time was measured after a drop of blood had been placed on each slide (Ramesh et al., 2021).

### Hemolysis Assay

The hemolysis assay involved preparing a fresh blood dilution of 1:10 PBS. Samples were added to 100 µl of blood and 1.5 ml of 1X PBS, incubated at 37°C for 2 h, and absorbance measured at 540 nm, with deionized water as a positive control and DMSO as a negative control (Slowing et al., 2009).

## Results

The synthesized ZnO and rGO-ZnO composite samples underwent ultrasonical dispersion in deionized water for 20 minutes. The development of the composite led to the appearance of absorption peaks at 243 nm and 366 nm for the rGO-ZnO composite (Fig. 4). The combination demonstrated band edge absorption at 366 nm, which is 18 nm less blue-shifted compared to bulk ZnO. The ZnO sample had a clear excitonic peak at 384 nm, which meant it was active in the UV and visible light ranges, as shown in Fig. 4. The ZnO spectra exhibited a distinct excitonic peak at 384 nm, indicating activity in the ultraviolet and visible light regions.

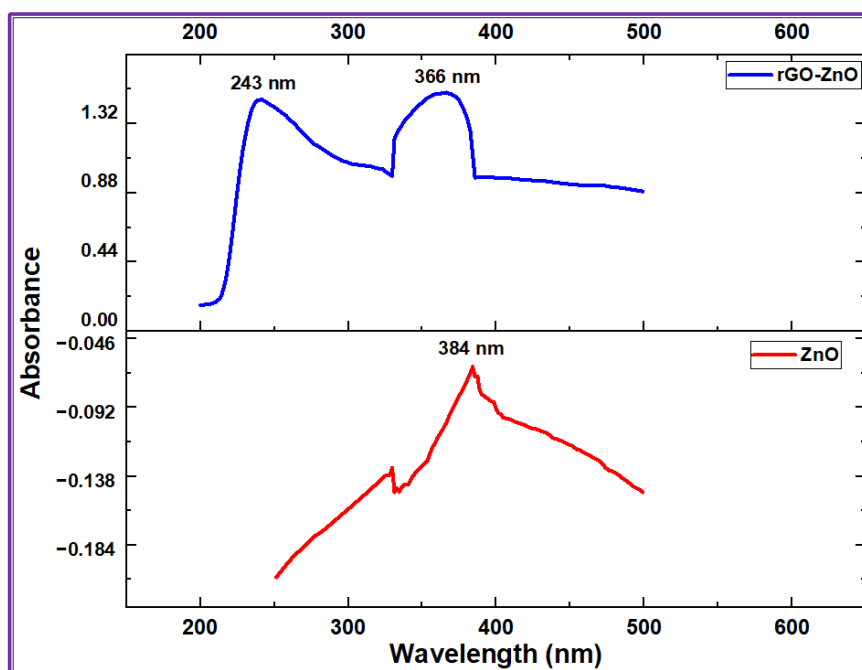


**Figure 4:** UV Absorbance of Synthesized ZnO from *I. coccinia* and Reduced Graphene Oxide Synthesis from *P. juliflora*

### Xrd Analysis

The X-ray diffraction analysis of the produced ZnO nanoparticles reveals an amorphous wurtzite structure with peaks at 31.54°, 34.22°, and 36.08°. In contrast, the rGO-ZnO composite XRD pattern reveals prominent peaks at 21.25°, 21.56°, 23.14°, and at 31.74°, 33.24°, 34.29°, and 36.23°, as illustrated in Fig. 5. We calculated the average particle sizes of ZnO and rGO-ZnO composite samples

using the Debye-Scherrer equation, yielding values of 37.35 nm and 41.77 nm, respectively. XRD patterns of the zinc oxide nanoparticles that were made showed a unique wurtzite structure, with clear peaks at  $31.54^\circ$ ,  $34.22^\circ$ , and  $36.08^\circ$ .

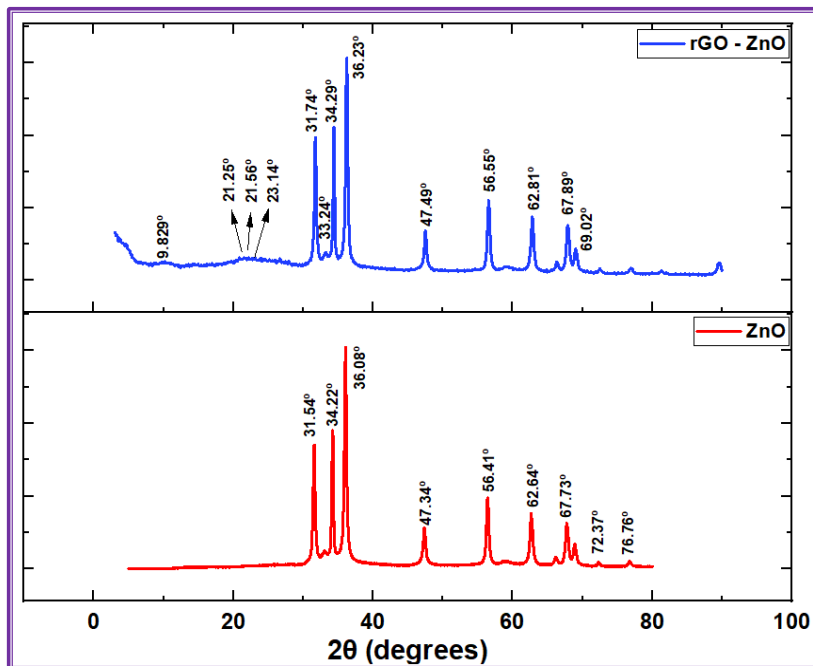


**Figure 5:** XRD Spectrum of Synthesized ZnO From *I. Coccinia* and Reduced Graphene Oxide Synthesis from *P. Juliflora*

#### FT-IR Analysis

The FT-IR spectra of ZnO and rGO-ZnO composites show distinct peaks that correspond to OH stretching, symmetric and antisymmetric stretching of  $\text{CH}_2$ , and aromatic groups. The peaks exhibit notable intensity changes attributed to the ZnO coating on the rGO surface. The OH stretching vibrations account for the significant absorption observed between  $3000$  and  $3500\text{ cm}^{-1}$  (Fig. 6).

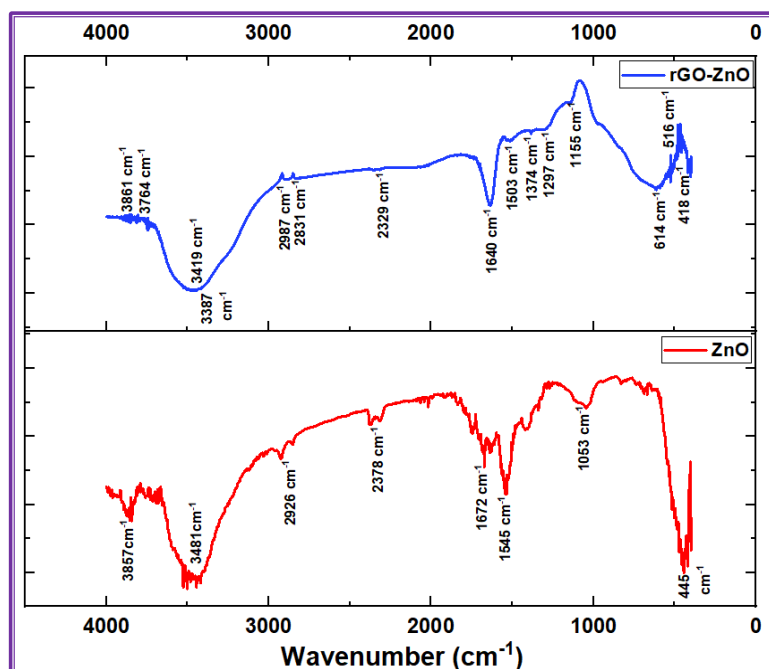
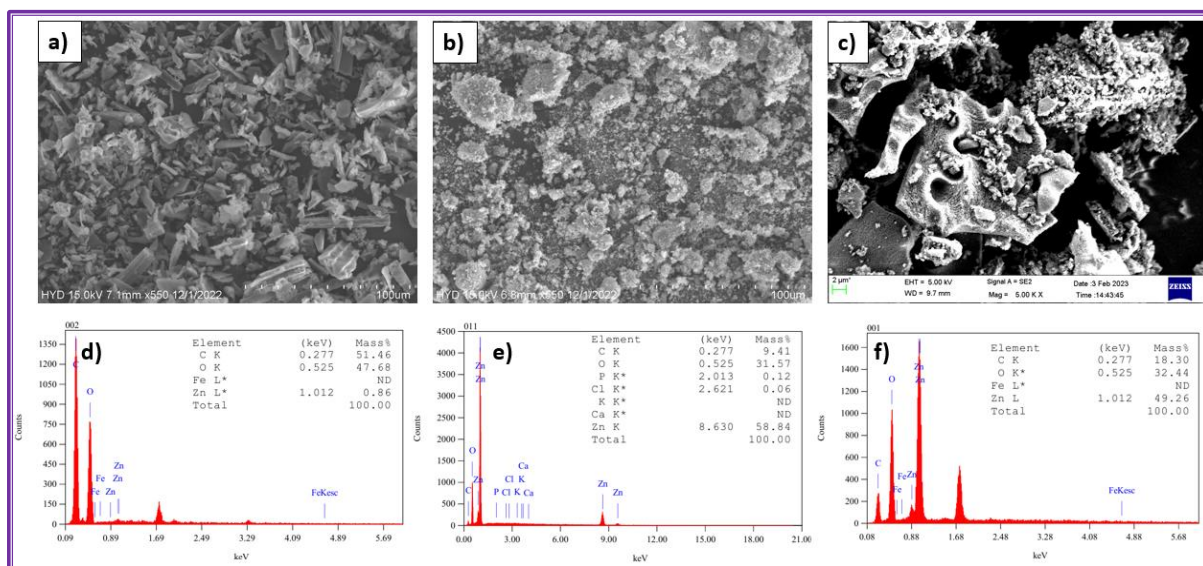


**Figure 6:** FTIR Spectra Synthesized ZnO from *I. coccinia* and Reduced Graphene Oxide Synthesis from *P. juliflora*

Sem-Edx Analysis

The surface morphology of the produced materials was analyzed using scanning electron microscopy in conjunction with energy dispersive X-ray spectroscopy. Fig. 7(a) displayed rod-like structures of reduced graphene oxide (rGO). Fig. 7(b) displayed densely clustered aggregates of ZnO. Fig 7(c) exhibited a reduced number of aggregated clusters adhered to a monolayer of the rGO-ZnO composite. EDX scans of the figures confirmed the elemental composition. Figs. 7(d), 7(e), and 7(f) of rGO, ZnO, and the rGO-ZnO composite show that the rGO-ZnO composite has a high zinc concentration of 49.26%, which means that magnetic stirring was used to achieve an effective loading rate. The elevated zinc concentration resulted from the effective integration of ZnO on the rGO surface, aided by magnetic stirring during synthesis.



**Figures 7: a-c. SEM of rGO, ZnO and rGO – ZnO; 7 d-f. EDX of rGO, ZnO and rGO – ZnO Composite Samples FTIR Spectra of ZnO and rGO – ZnO Composite Samples**

Antioxidant Activity

The DPPH assay assessed the effectiveness of synthesized ZnO and rGO-ZnO samples in scavenging free radicals. Compared to regular ascorbic acid, the rGO-ZnO compound had a strong scavenging effect. At a dose of 400 µg/ml, the purple color completely disappeared. Fig. 8 shows that both ZnO and rGO-ZnO samples had free radical-scavenging properties, with higher concentrations showing more scavenging activity.

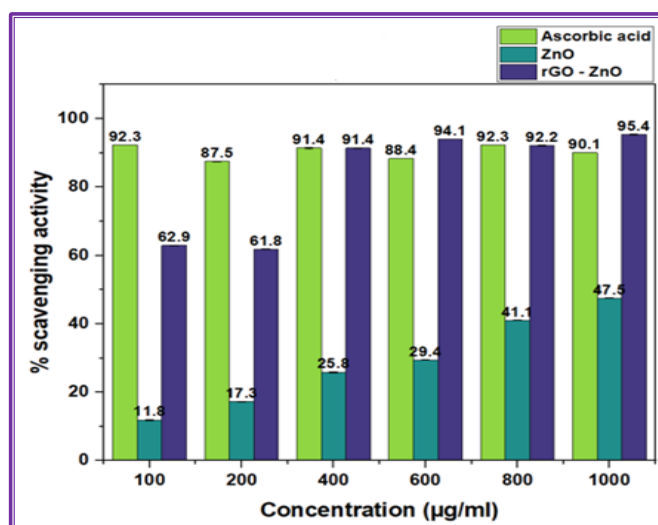


**Figure 8: Free Radical Scavenging Activities of Synthesized ZnO and rGO - ZnO Samples**

Antibacterial Activity

The antibacterial efficacy of biosynthesized ZnO and rGO-ZnO composite samples against Gram-negative (*E. coli*) and Gram-positive (*B. subtilis*) bacteria using the disc diffusion method. The result indicated that the levels of ZnO and rGO-ZnO escalated alongside the zone of inhibition. The figure 9 illustrates ampicillin acting as a positive control, likely due to enhanced metal ion penetration and disruption of the bacterial cell membrane, which in turn affects cellular processes. The rGO-ZnO composite's zone of inhibition against Gram-positive (*B. subtilis*) was about 1.5 cm across at 80 µl. Conversely, in Gram-negative bacteria (*E. coli*), the inhibitory zone expands with rising concentration, as illustrated in Fig. 10.

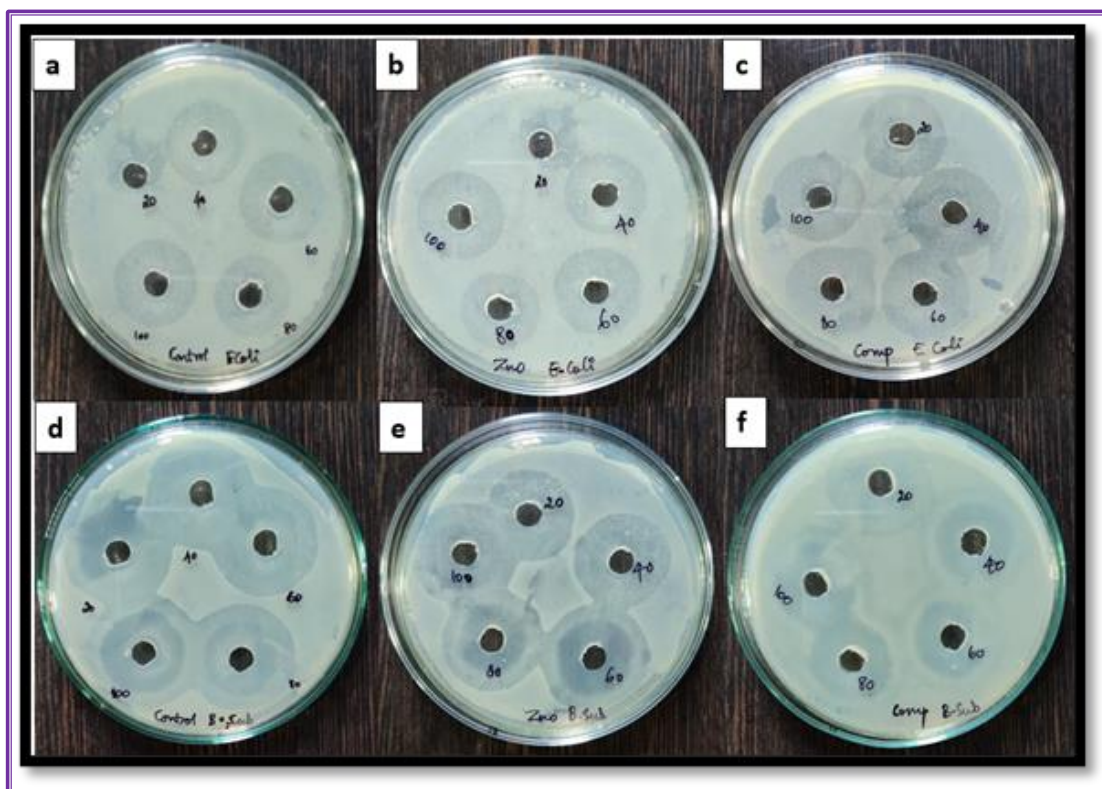


Figure 9: Antibacterial Activity of (a) Ampicillin (b) ZnO (c) rGO – ZnO Composite on *E. coli* and (d) Ampicillin (e) ZnO (f) rGO – ZnO Composite Samples on *B. Subtilis*

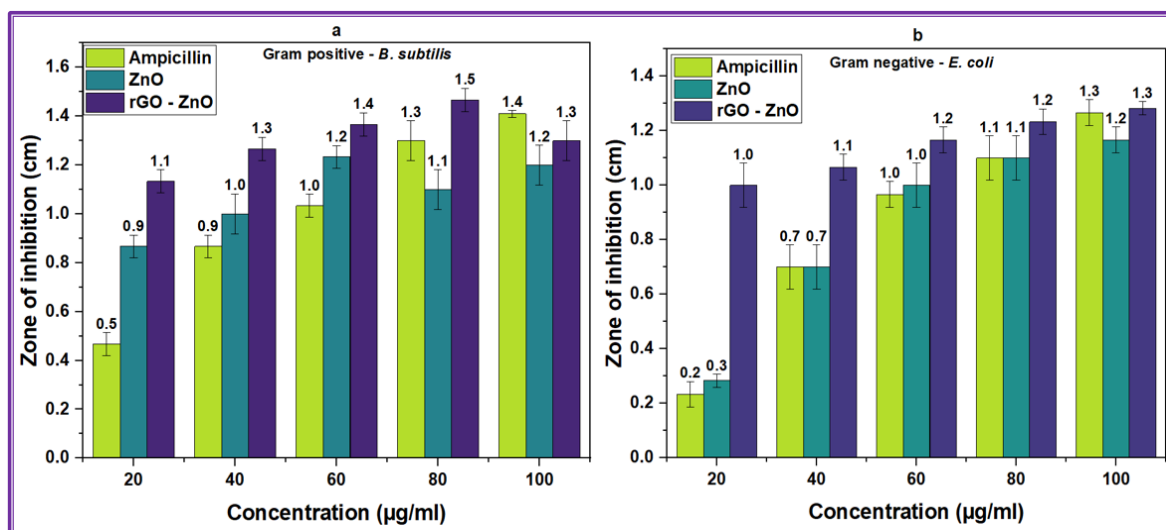
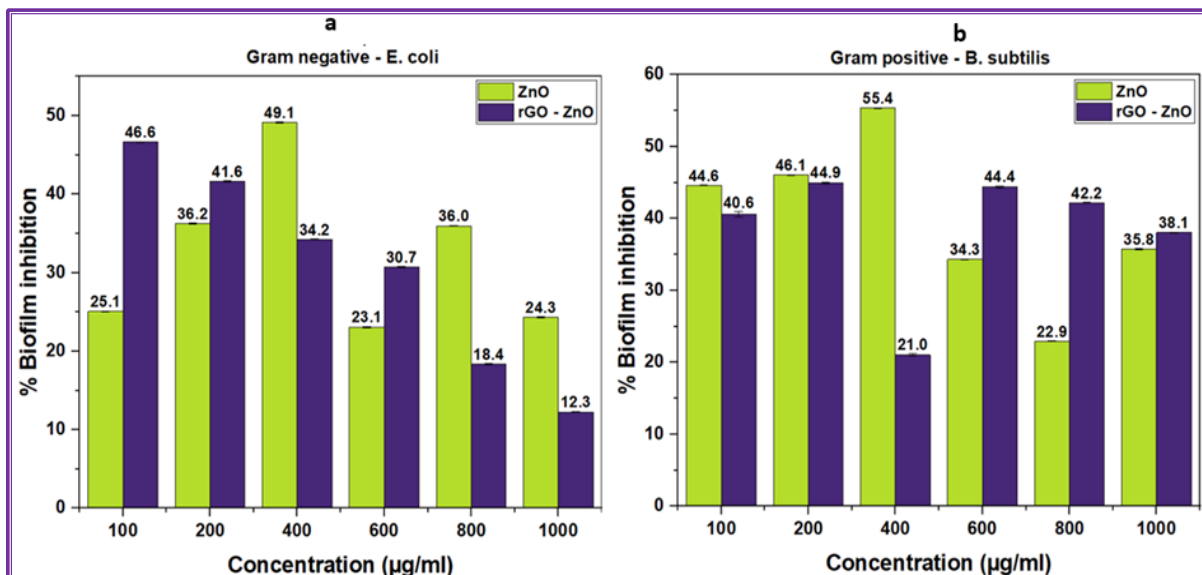


Figure 10: Zone of inhibition of (a) *B. Subtilis* and (b) *E. coli* on Ampicillin, ZnO, and rGO – ZnO Composite

**Biofilm Inhibition Activity**

The rGO-ZnO compound significantly suppressed the biofilm activity of Gram-negative *E. coli*, exhibiting a marked antibacterial activity against this pathogen. *E. coli* diminished with higher concentrations, demonstrating 47% biofilm inhibition at 100 µg/ml (Fig. 11a). *B. subtilis* exhibited considerable antibacterial efficacy, diminishing biofilm formation by as much as 45% at a concentration of 200 µg/ml (Fig. 11b). Both ZnO and the rGO-ZnO composite exhibited remarkable antibacterial efficacy at reduced doses. We employed the crystal violet assay to assess the effect of ZnO and rGO-ZnO composites on biofilm inhibition in both Gram-negative and Gram-positive bacteria.



**Figure 11:** Inhibition Percentage of (a) *E. coli* and (b) *B. Subtilis* Biofilm Using ZnO and rGO-ZnO Anti-Inflammatory Activity

The study examined the anti-inflammatory efficacy of ZnO and rGO-ZnO composites at various doses, using aceclofenac as a control. Both compounds showed they could stop albumin from breaking down, but the rGO-ZnO composite was the most effective, showing 93% activity at concentrations as high as 400 µg/ml (Fig. 12).

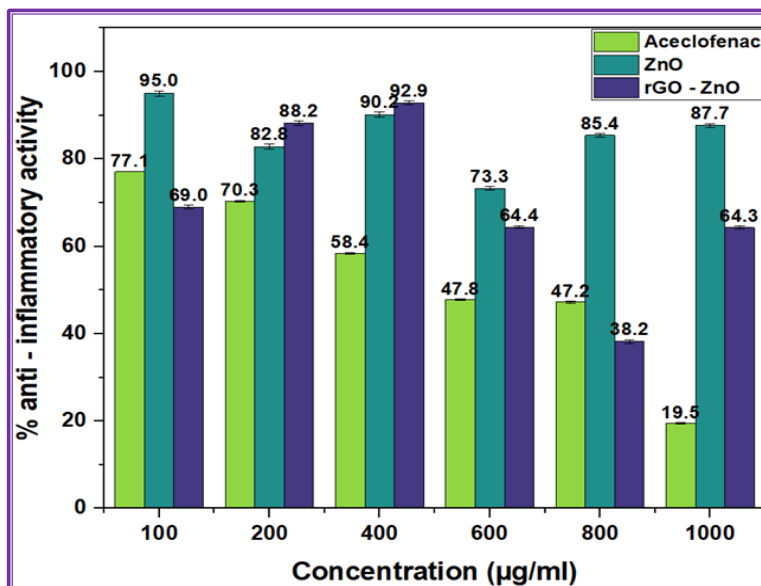


**Figure 12:** Anti-inflammatory Activity of Aceclofenac, ZnO and rGO-ZnO Anti-Diabetic Activity

The anti-diabetic effectiveness of ZnO and rGO-ZnO composite samples in yeast cells at varying glucose concentrations. The results indicated an absence of dosage-dependent glucose absorption, with elevated uptake at 100 µg/ml and a decline at higher concentrations (Fig. 13). ZnO and rGO-ZnO composites exhibited consistent efficacy across all glucose values, surpassing metformin in performance.

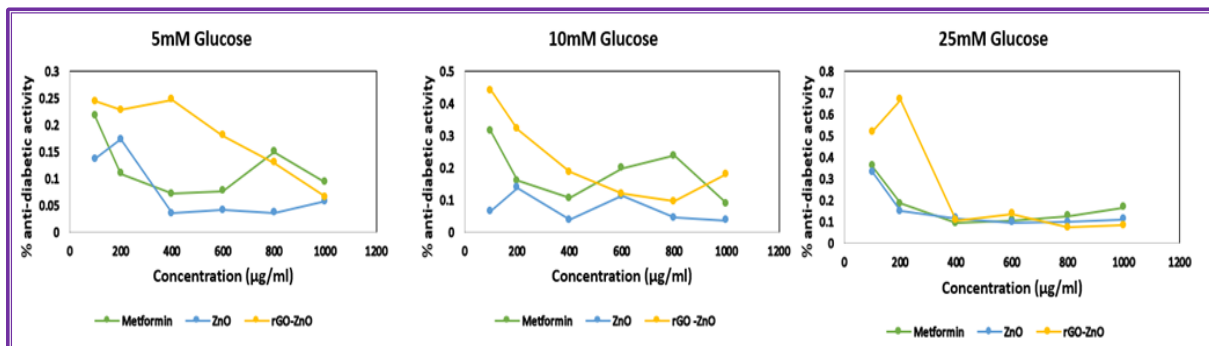


**Figure 13:** Anti-diabetic Activity of Metformin, ZnO and rGO-ZnO in 5mM, 10mM, and 25 mM Glucose Concentrations

**Hemolysis Activity**

Human blood samples were procured from Karpaga Vinayaga Institute of Medical Sciences and Research Centre, Chengalpattu, Tamil Nadu, for research purposes, ensuring that all ethical and biosafety regulations were followed as per Institutional Human Ethical Committee approved protocols. Studies on biocompatibility and hemolytic activity assay using ZnO and rGO-ZnO composite materials, demonstrate hemocompatibility with human RBC cells (PP 2020). Fig. 14 demonstrate that samples exhibit essentially consistent hemolysis proportions up to 400 µg/ml. The rGO-ZnO composite demonstrated enhanced biocompatibility and a reduced hemolysis percentage of 0.5% (Fig. 15).

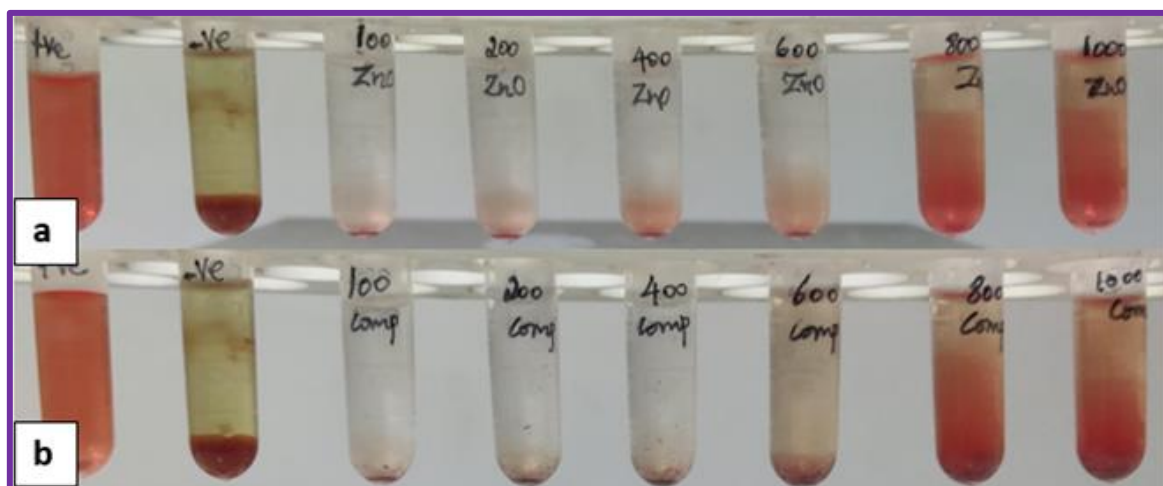


**Figure 14:** Hemolysis activity of (a) ZnO and (b) rGO – ZnO Composite Samples

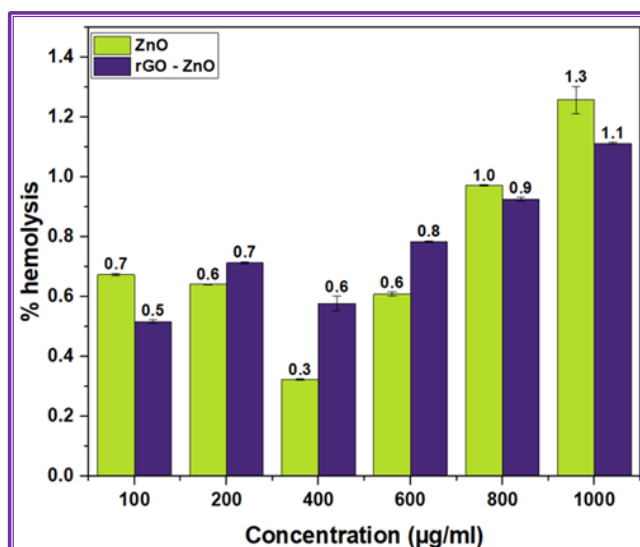


**Figure 15:** Hemolysis Percentage Using ZnO and rGO-ZnO

#### Anticoagulation Assay

The anticoagulation assay was used to investigate the anticoagulant properties of ZnO and rGO-ZnO composite materials in human blood. The results showed that the synthesized ZnO and the rGO-ZnO composite made the blood less likely to clot. Clots formed at the 7th and 20th minutes, respectively (Fig. 16).

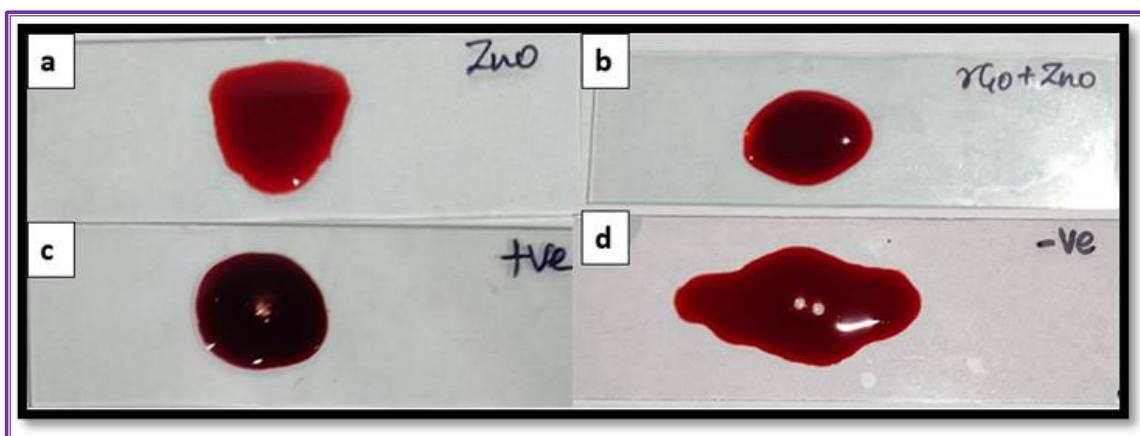


**Figure 16:** Anti-Coagulation Activity of (a) ZnO, (b) rGO – ZnO Composite, (c) Positive Control, (d) Negative Control

#### Discussion

The appearance of absorption peaks at 243 nm and 366 nm shows that the rGO-ZnO composite was successfully made and mixed with zinc oxide (ZnO). The peak at 366 nm signifies a band-edge absorption feature of ZnO. This information is supported by studies conducted by Potbhare *et al.* (2024). The absorbance peak at 243 nm is due to the  $\pi \rightarrow \pi^*$  transitions of rGO. This shows that graphene oxide helps keep the ZnO particles in the composite stable. The rGO-ZnO composite has two different peaks in the UV-Vis spectrum. These peaks show how the electronic properties of rGO and ZnO interact, which improves the photocatalytic performance of the composite, which is supported by other studies (Ahmed & Haider 2021; Landström *et al.*, 2021). The strong excitonic peak at 384 nm in the pure ZnO sample shows that it can absorb UV light, which is important for photocatalytic uses and processes that are driven by UV light. The coexistence of UV and visible light activity in the rGO-ZnO composite enhances its use in environmental remediation and energy conversion. The similar results reported (Zhang *et al.* 2020) that mixing graphene materials with metal oxides makes it easier to separate and

transfer charges, which makes photocatalysis work better. Recent studies have focused on the synthesis and characterization of ZnO nanoparticles, which have attracted considerable interest because of their distinctive features and possible applications in diverse disciplines such as catalysis, sensors, and photonics. The synthesized *I. coccinia* ZnO nanoparticles are amorphous, as shown by the clear peaks at 31.54°, 34.22°, and 36.08°. The peaks that were found exactly match the known diffraction peaks of ZnO from the literature, especially from Joseph & Poornima (2019), who found similar peak positions for the hexagonal wurtzite phase. The *P. juliflora* rGO-ZnO composite exhibited pronounced peaks at 21.25°, 21.56°, 23.14°, 31.74°, 33.24°, 34.29°, and 36.23°. The appearance of these peaks shows that Reduced Graphene Oxide (rGO) and ZnO are interacting in a planned way, which makes the composite's structural properties better. This finding is supported by a study by Liu *et al.* (2019), which shows that structures that combine reduced graphene oxide (rGO) with metal oxides improve crystallinity and phase stability. This is because rGO and ZnO work together to make these structures stronger.

The Debye-Scherrer equation showed that the average particle sizes for ZnO were 37.35 nm and for the rGO-ZnO composite they were 41.77 nm. (Pal *et al.*, 2019) found that ZnO particles have sizes between 30 and 50 nm. They emphasized that the synthesis parameters could be changed to make particle sizes fit specific needs. The integration of rGO, which may affect the growth dynamics of the nanoparticles during synthesis, is responsible for the marginal increase in size of the rGO-ZnO composite. The results highlight the adaptability and potential applications of ZnO and its composites, especially in improving optical and electrical properties by precisely controlling particle size and structural configuration. This study enhances the existing information regarding the synthesis and characterization of metal oxide nanocomposites for advanced applications. To contextualize the results, it is essential to compare the surface morphology and elemental content of the synthesized rGO-ZnO composite with earlier investigations.

The zinc content of 49.26% in the rGO-ZnO composite corresponds with similar studies, which indicated that successful synthesis processes permit increased metal loading onto reduced graphene oxide (rGO). Zhang *et al.* (2020) stated it that showed how changing synthesis parameters, like the speed and length of stirring, had a big effect on how much metal oxide could be loaded onto rGO substrates. Their findings indicate a ZnO loading of up to 50% on rGO under optimum conditions, corroborating the high zinc content seen in the current work. Zhang *et al.* (2020) attribute the results to the enhanced presence of surface functional groups on rGO, which facilitate interactions with metal oxides, thereby fostering improved dispersion and uniformity. Also, the morphological studies based on the Scanning Electron Microscopy (SEM) images show that the rod-like structures of ZnO mixed with rGO can improve the way electrons interact with each other. Marlinda *et al.* (2019) looked at similar morphological aspects and showed that the unique geometrical structures of ZnO can improve charge transfer properties when used with graphene-based materials, leading to better photocatalytic activity.

The DPPH experiment was a well-known way to test how well different chemicals, including those from natural sources and nanocomposites, can get rid of free radicals. In the present study, *I. coccinia* ZnO was synthesized and *P. juliflora* rGO-ZnO samples were very good at neutralizing DPPH radicals, which is a sign of strong antioxidant activity. The graphene-based composites, especially those with metal oxides, were better at scavenging free radicals because they have more surface area and can donate electrons (Baali *et al.*, 2019). The distinctive characteristics of Reduced Graphene Oxide (rGO) promote effective interaction with free radicals, thereby augmenting the overall antioxidant capacity. On the other hand, both ZnO and rGO-ZnO samples had free radical scavenging abilities that depended on their concentration, with higher sample concentrations showing higher scavenging activity. Previous study has indicated analogous concentration-dependent tendencies in the scavenging activities of nanoparticles and nanocomposites (Caponio *et al.*, 2022) found that the antioxidant activity of natural extracts usually goes up with concentration. This is because free radicals and antioxidant molecules are more likely to interact with each other. The rGO-ZnO composite was better at scavenging free radicals than regular ascorbic acid, which is a well-known antioxidant. On the other hand, ZnO alone was not as good. This observation may be associated with the unique methods of action and the

structural characteristics of the materials involved. Ascorbic acid donates hydrogen and can effectively neutralize free radicals. However, adding rGO to the ZnO structure seems to improve the overall electron transfer process, which makes radical scavenging more effective.

Sirelkhatim *et al.* (2015) showed that zinc oxide nanoparticles have very good antibacterial activity against both Gram-positive and Gram-negative bacteria. Sportelli *et al.* (2022) stated that nanomaterials may not work as well against Gram-positive and Gram-negative organisms because their cell walls are made of different chemicals. *B. subtilis* thicker peptidoglycan layer typically makes it more resistant to certain antimicrobial drugs compared to the thinner cell wall of *E. coli*. Sirelkhatim *et al.* (2015) observed similar trends in their research on ZnO nanoparticles and proposed a complex interaction among concentration, bacterial exposure, and potential resistance. Different doses of the rGO-ZnO composite in this study showed different levels of effectiveness in reducing biofilm formation in both Gram-negative and Gram-positive bacteria. *Sesbania grandiflora* leaf extracts against the bacterial strains of *E. coli*, *Staphylococcus aureus*, *Streptococcus oralis*, and *Pseudomonas aeruginosa* showed significant inhibition zone between the different concentrations (50 µg/ml, 100 µg/ml, 250 µg/ml, and 500 µg/ml) (Mani *et al.*, 2025).

The significant inhibition observed with *E. coli* in biofilm formation decreased by 47% at 100 µg/mL, corroborating earlier research that underscores the antibacterial efficacy of ZnO-based composites. Gudkov *et al.* (2021) demonstrated that ZnO nanoparticles have shown considerable anti-biofilm efficacy against *E. coli*. The effect on the production of Reactive Oxygen Species (ROS) and the compromise of the bacterial cell membrane. Similarly, they reported a 45% decrease in biofilm formation. (Rajapaksha *et al.*, 2023) stated that adding reduced graphene oxide (rGO) to ZnO increased the bioactivity of ZnO and made the composite more stable and easier to disperse, which in turn increased its effectiveness. The researchers stressed that the synergistic interaction between rGO and ZnO in their study made it easier for bacteria to absorb ZnO, which made it more effective as an antibacterial activity than ZnO alone. In the present study, the antibacterial activity dropped as the concentration of the rGO-ZnO composite increased. This could be a sign of a threshold effect or possible harm at higher doses (Sirelkhatim *et al.*, 2015) indicated that, although nanoscale ZnO efficiently suppressed biofilm formation, excessively high concentrations could adversely affect both the targeted bacterial cells and adjacent mammalian cells, consequently diminishing overall antibacterial efficacy.

This study investigates the anti-diabetic effectiveness of ZnO and reduced graphene oxide (rGO)-ZnO composite samples in *S. cerevisiae*. This study investigates how *S. cerevisiae* responds to various glucose concentrations. The results indicate notable patterns in glucose absorption, particularly at a concentration of 100 µg/ml, where substantial uptake was recorded. At greater doses, glucose absorption decreased, suggesting a potential saturation effect or cytotoxicity at high dosages. In the present study, results differ from other research examining the effects of metal oxides and their composites on glucose metabolism. Numerous results indicate that nanomaterials can improve glucose absorption in numerous cell types, such as pancreatic β-cells and muscle cells (Wahba *et al.*, 2016; Gaikwad *et al.*, 2023). It is crucial to emphasize that, although we noted substantial glucose uptake at lower doses, elevated concentrations of ZnO and rGO-ZnO induced a decline in activity. The similar results were reported by Czyżowska & Barbasz (2021), which showed that too much ZnO exposure might lead to oxidative stress and cell damage, which would make metabolism work less well. rGO-ZnO composites signify a notable progression in the quest for innovative anti-diabetic medicines, exhibiting substantial effectiveness in enhancing glucose absorption in yeast cells relative to conventional therapy. Further examination of the safety and mechanism of action is crucial to fully exploiting their medicinal potential.

## Conclusion

The present investigation utilized *I.coccinia* flower extract makes the non-toxic, quick, cheap, and long-lasting synthesis of ZnO possible. The rGO-ZnO combination has significant activity within the concentration range of 100 to 400 µg/ml for most assays conducted. We evaluated the rGO-ZnO

composite for its efficacy in inhibiting biofilm formation, which demonstrated a substantial inhibitory zone against both gram-positive and gram-negative species. The hemolytic activity of the rGO-ZnO composite was found to be inferior to that of human RBC lysis, but it did exhibit commendable free radical scavenging capacity, along with pronounced anti-inflammatory and anti-diabetic properties, demonstrating a substantial difference. Researchers have recognized the integration of reduced graphene oxide (rGO) as a matrix with zinc oxide (ZnO) nanostructures as a potential material for highly selective and sensitive biomedical applications. The distinctive characteristics of ZnO nanoparticles, including low toxicity and biodegradability, render them appropriate for biological applications. The investigation is focused on rGO-ZnO nanocomposites that utilize *I. coccinea* and *P. juliflora* has a lot of potential because the two substances work well together to improve therapeutic properties and biocompatibility. The application of *I. coccinea* shows great commercial and translational potential. Its availability, low cost, and overall phytochemistry are advantageous; it has the potential to fulfill sustainable nanomaterial synthesis. The use of green, nontoxic chemical reducing agents fits well with the philosophic tenets of green chemistry and environmentally conscious advanced manufacturing.

### Conflict of Interest

The authors declare that they have no competing interests.

### Acknowledgement

The authors (AAC, KRP) express their gratitude to the Management, Principal, and Head of the Department of Biotechnology at St. Joseph's College of Engineering, Chennai, for their facilitation of laboratory access for this work. The authors (AAC, KSK, and SVM) express gratitude to the Management, Principal, and Head of the Department of Biotechnology, Karpaga Vinayaga College of Engineering and Technology, Chengalpattu, for their continued support in completing the research effort.

### References

- Abdelfatah, A. M., El-Maghrabi, N., Mahmoud, A. E. D., & Fawzy, M. (2022). Synergetic effect of green synthesized reduced graphene oxide and nano-zero valent iron composite for the removal of doxycycline antibiotic from water. *Scientific Reports*, 12(1), 19372. <https://doi.org/10.1038/s41598-022-23684-x>
- Ahamed, M., Akhtar, M. J., & Khan, M. M. (2020). Investigation of cytotoxicity, apoptosis, and oxidative stress response of Fe<sub>3</sub>O<sub>4</sub>-RGO nanocomposites in human liver HepG2 cells. *Materials*, 13(3), 660. <https://doi.org/10.3390/ma13030660>
- Ahamed, M., Akhtar, M. J., Khan, M. M., & Alhadlaq, H. A. (2021). SnO<sub>2</sub>-doped ZnO/reduced graphene oxide nanocomposites: synthesis, characterization, and improved anticancer activity via oxidative stress pathway. *International Journal of Nanomedicine*, 16, 89-104. <https://doi.org/10.2147/ijn.s285392>
- Ahmed, S. N., & Haider, W. (2021). Enhanced photocatalytic activity of ZnO-graphene oxide nanocomposite by electron scavenging. *Catalysts*, 11(2), 187. <https://doi.org/10.3390/catal11020187>
- Baali, N., Khecha, A., Bensouici, A., Speranza, G., & Hamdouni, N. (2019). Assessment of antioxidant activity of pure graphene oxide (GO) and ZnO-decorated reduced graphene oxide (rGO) using DPPH radical and H<sub>2</sub>O<sub>2</sub> scavenging assays. *C*, 5(4), 75. <https://doi.org/10.3390/c5040075>
- Baliga, M. S., & Kurian, P. J. (2012). *Ixora coccinea* Linn.: Traditional uses, phytochemistry and pharmacology. *Chinese journal of integrative medicine*, 18(1), 72-79. <https://doi.org/10.1007/s11655-011-0881-3>
- Balouiri, M., Sadiki, M., & Ibensouda, S. K. (2016). Methods for in vitro evaluating antimicrobial activity: A review. *Journal of Pharmaceutical Analysis*, 6(2), 71-79. <https://doi.org/10.1016/j.jpha.2015.11.005>
- Bandeira, M., Giovanela, M., Roesch-Ely, M., Devine, D. M., & da Silva Crespo, J. (2020). Green synthesis of zinc oxide nanoparticles: A review of the synthesis methodology and mechanism of formation. *Sustainable Chemistry and Pharmacy*, 15, 100223. <https://doi.org/10.1016/j.scp.2020.100223>
- Banu, K. S., & Cathrine, L. (2015). General techniques involved in phytochemical analysis. *International Journal of Advanced Research in Chemical Science*, 2(4), 25-32. <https://www.arcjournals.org/pdfs/ijarcs/v2-i4/5.pdf>
- Barui, A. K., Kotcherlakota, R., & Patra, C. R. (2018). Biomedical applications of zinc oxide nanoparticles. In *Inorganic frameworks as smart nanomedicines* (pp. 239-278). William Andrew Publishing. <https://doi.org/10.1016/B978-0-12-813661-4.00006-7>

- Bozetine, H., Wang, Q., Barras, A., Li, M., Hadjersi, T., Szunerits, S., & Boukherroub, R. (2016). Green chemistry approach for the synthesis of ZnO–carbon dots nanocomposites with good photocatalytic properties under visible light. *Journal of Colloid and Interface Science*, 465, 286-294. <https://doi.org/10.1016/j.jcis.2015.12.001>
- Burits, M., & Bucar, F. (2000). Antioxidant activity of *Nigella sativa* essential oil. *Phytotherapy Research*, 14(5), 323-328. [https://doi.org/10.1002/1099-1573\(200008\)14:5%3C323::aid-ptr621%3E3.0.co;2-q](https://doi.org/10.1002/1099-1573(200008)14:5%3C323::aid-ptr621%3E3.0.co;2-q)
- Campbell, E., Hasan, M. T., Pho, C., Callaghan, K., Akkaraju, G. R., & Naumov, A. V. (2019). Graphene oxide as a multifunctional platform for intracellular delivery, imaging, and cancer sensing. *Scientific reports*, 9(1), 416. <https://doi.org/10.1038/s41598-018-36617-4>
- Caponio, F., Piga, A., & Poiana, M. (2022). Valorization of food processing by-products. *Foods*, 11(20), 3246. <https://doi.org/10.3390/foods11203246>
- Chamundeeswari, M., & Preethy, K. R. (2024). Sustainable strategy of biowaste into graphene-based zinc oxide nanocomposite using green nanotechnology for topical applications. *Biotechnology and Applied Biochemistry*, 72(3). <https://doi.org/10.1002/bab.2702>
- Coroş, M., Pogăcean, F., Măgeruşan, L., Socaci, C., & Pruneanu, S. (2019). A brief overview on synthesis and applications of graphene and graphene-based nanomaterials. *Frontiers of Materials Science*, 13(1), 23-32. <https://doi.org/10.1007/s11706-019-0452-5>
- Czyżowska, A., & Barbasz, A. (2021). Cytotoxicity of zinc oxide nanoparticles to innate and adaptive human immune cells. *Journal of Applied Toxicology*, 41(9), 1425-1437. <https://doi.org/10.1002/jat.4133>
- Dar, A., Rehman, R., Zaheer, W., Shafique, U., & Anwar, J. (2021). Synthesis and characterization of ZnO-nanocomposites by utilizing aloe vera leaf gel and extract of *Terminalia arjuna* nuts and exploring their antibacterial potency. *Journal of Chemistry*, 2021(1), 9448894. <https://doi.org/10.1155/2021/9448894>
- De Matteis, V., Cascione, M., Rizzello, L., Liatsi-Douvitsa, E., Apriceno, A., & Rinaldi, R. (2020). Green synthesis of nanoparticles and their application in cancer therapy. In *Green synthesis of nanoparticles: Applications and prospects* (pp. 163-197). Singapore: Springer Singapore. [https://doi.org/10.1007/978-981-15-5179-6\\_8](https://doi.org/10.1007/978-981-15-5179-6_8)
- Dey, P., Chatterjee, P., Chandra, S., & Bhattacharya, S. (2011). Comparative in vitro evaluation of anti-inflammatory effects of aerial parts and roots from *Mikania scandens*. *Journal of Advanced Pharmacy Education & Research*, 1(6), 269-277. <https://japer.in/storage/models/article/wHeqPuNLHOZZ88U4UIAJ3zLXUwMFXDj8PTHNzzmaHZf4bnmPZDuzl8kLhznk/comparative-in-vitro-evaluation-of-anti-inflammatory-effects-of-aerial-parts-and-roots-from-mikani.pdf>
- Dontha, S., Kamurthy, H., & Mantripragada, B. (2015). Phytochemical and pharmacological profile of *Ixora*: a review. *International Journal of Pharmaceutical Sciences and Research*, 6(2), 567-584. [http://dx.doi.org/10.13040/IJPSR.0975-8232.6\(2\).567-84](http://dx.doi.org/10.13040/IJPSR.0975-8232.6(2).567-84)
- Durmus, Z., Kurt, B. Z., & Durmus, A. (2019). Synthesis and characterization of graphene oxide/zinc oxide (GO/ZnO) nanocomposite and its utilization for photocatalytic degradation of basic fuchsin dye. *ChemistrySelect*, 4(1), 271-278. <https://doi.org/10.1002/slct.201803635>
- Elbasuney, S., El-Sayyad, G. S., Tantawy, H., & Hashem, A. H. (2021). Retracted article: promising antimicrobial and antibiofilm activities of reduced graphene oxide-metal oxide (RGO-NiO, RGO-AgO, and RGO-ZnO) nanocomposites. *RSC advances*, 11(42), 25961-25975. <https://doi.org/10.1039/D1RA04542C>
- Gaikwad, S., Vora, S., Bansode, A., Garje, V., Bhaiya, S., & Choudhari, V. (2023). Green synthesis of metal oxide nanoparticles: A novel approach to treat diabetes mellitus. *BioNanoScience*, 13(4), 1582-1592. <https://dx.doi.org/10.2139/ssrn.4073643>
- Garaj, S., Hubbard, W., Reina, A., Kong, J., Branton, D., & Golovchenko, J. A. (2010). Graphene as a subnanometre trans-electrode membrane. *Nature*, 467(7312), 190-193. <https://doi.org/10.1038/nature09379>
- Gudkov, S. V., Burmistrov, D. E., Serov, D. A., Rebezov, M. B., Semenova, A. A., & Lisitsyn, A. B. (2021). A mini review of antibacterial properties of ZnO nanoparticles. *Frontiers in Physics*, 9, 641481. <https://doi.org/10.3389/fphy.2021.641481>
- Haghighi, B., & Tabrizi, M. A. (2013). Green-synthesis of reduced graphene oxide nanosheets using rose water and a survey on their characteristics and applications. *RSC Advances*, 3(32), 13365-13371. <https://doi.org/10.1039/c3ra40856f>
- Hussein, A. H., & Yassir, Y. A. (2024). Development of a graphene oxide/hydroxyapatite-containing orthodontic primer: An in-vitro study. *Materials Chemistry and Physics*, 326, 129857. <https://doi.org/10.1016/j.matchemphys.2024.129857>
- Ilie, N., Serfoezoe, N. E., Prodan, D., Diegelmann, J., & Moldovan, M. (2022). Synthesis and performance of experimental resin-based dental adhesives reinforced with functionalized graphene and hydroxyapatite fillers. *Materials & Design*, 221(7), 110985. <https://doi.org/10.1016/j.matdes.2022.110985>

- Jadoun, S., Arif, R., Jangid, N. K., & Meena, R. K. (2021). Green synthesis of nanoparticles using plant extracts: A review. *Environmental Chemistry Letters*, 19, 355-374. <https://doi.org/10.1007/s10311-020-01074-x>
- Joseph, H. M., & Poornima, N. (2019). Synthesis and characterization of ZnO nanoparticles. *Materials Today: Proceedings*, 9(Part 1), 7-12. <https://doi.org/10.1016/j.matpr.2019.02.029>
- Kalpna, V. N., & Rajeswari, V. D. (2018). A review on green synthesis, biomedical applications, and toxicity studies of ZnO NPs. *Bioinorganic Chemistry and Applications*, 2018(1), 3569758. <https://doi.org/10.1155/2018/3569758>
- Khorasani, M. T., Joorabloo, A., Moghaddam, A., Shamsi, H., & MansooriMoghaddam, Z. (2018). Incorporation of ZnO nanoparticles into heparinised polyvinyl alcohol/chitosan hydrogels for wound dressing application. *International Journal of Biological Macromolecules*, 114, 1203-1215. <https://doi.org/10.1016/j.ijbiomac.2018.04.010>
- Landström, A., Gradone, A., Mazzaro, R., Morandi, V., & Concina, I. (2021). Reduced graphene oxide-ZnO hybrid composites as photocatalysts: the role of nature of the molecular target in catalytic performance. *Ceramics International*, 47(14), 19346-19355. <https://doi.org/10.1016/j.ceramint.2021.03.271>
- Li, B., Liu, T., Wang, Y., & Wang, Z. (2012). ZnO/graphene-oxide nanocomposite with remarkably enhanced visible-light-driven photocatalytic performance. *Journal of Colloid and Interface Science*, 377(1), 114-121. <https://doi.org/10.1016/j.jcis.2012.03.060>
- Lin, F., Li, C., & Chen, Z. (2018). Bacteria-derived carbon dots inhibit biofilm formation of *Escherichia coli* without affecting cell growth. *Frontiers in Microbiology*, 9, 259. <https://doi.org/10.3389/fmicb.2018.00259>
- Liu, W. M., Li, J., & Zhang, H. Y. (2020). Reduced graphene oxide modified zinc oxide composites synergistic photocatalytic activity under visible light irradiation. *Optik*, 207, 163778. <https://doi.org/10.1016/j.jileo.2019.163778>
- Luque, P. A., Soto-Robles, C. A., Nava, O., Gomez-Gutierrez, C. M., Castro-Beltran, A., Garrafa-Galvez, H. E., ... & Olivas, A. (2018). Green synthesis of zinc oxide nanoparticles using *Citrus sinensis* extract. *Journal of Materials Science: Materials in Electronics*, 29(12), 9764-9770. <https://doi.org/10.1007/s10854-018-9015-2>
- Majeed, S., Joel, E. L., & Hasnain, M. S. (2018). Novel green approach for synthesis of metallic nanoparticles and its biomedical application. *Current Nanomedicine (Formerly: Recent Patents on Nanomedicine)*, 8(3), 177-183. <https://doi.org/10.2174/2468187308666180301142158>
- Mandal, S. K., Dutta, K., Pal, S., Mandal, S., Naskar, A., Pal, P. K., ... & Jana, D. (2019). Engineering of ZnO/rGO nanocomposite photocatalyst towards rapid degradation of toxic dyes. *Materials Chemistry and Physics*, 223, 456-465. <https://doi.org/10.1016/j.matchemphys.2018.11.002>
- Mani, S. R., Valliappan, M. S., Dhandapani, D., Desamuthu, G., Ravichandran, M., Babu, B., & Kandhasamy S. (2025) Environmentally sustainable green synthesis of novel nano-hydroxyapatite derived from *Sesbania grandiflora* leaf and *Sesamum indicum* seed: *In Vitro* evaluation for dental restorative applications. *Next Materials* 8:100828. <https://doi.org/10.1016/j.nxmte.2025.100828>
- Marlinda, A. R., Yusoff, N., Pandikumar, A., Huang, N. M., Akbarzadeh, O., Sagadevan, S., ... & Johan, M. R. (2019). Tailoring morphological characteristics of zinc oxide using a one-step hydrothermal method for photoelectrochemical water splitting application. *International Journal of Hydrogen Energy*, 44(33), 17535-17543. <https://doi.org/10.1016/j.ijhydene.2019.05.109>
- Nasrollahzadeh, M., Sajjadi, M., Dasmeh, H. R., & Sajadi, S. M. (2018). Green synthesis of the Cu/sodium borosilicate nanocomposite and investigation of its catalytic activity. *Journal of Alloys and Compounds*, 763, 1024-1034. <https://doi.org/10.1016/j.jallcom.2018.05.012>
- Ostrovsky, S., Kazimirsky, G., Gedanken, & Broide, C. (2009). Selective cytotoxic effect of ZnO nanoparticles on glioma cells. *Nano Research*. 2, 882–890 (2009). <https://doi.org/10.1007/s12274-009-9089-5>
- Pal, S., Mondal, S., Pal, P., & Maity, J. (2019). Green synthesis, characterization and applications of ZnO nanoparticles—a review. *Advanced Science, Engineering and Medicine*, 11(11), 1009-1022. <https://doi.org/10.1166/ asem.2019.2532>
- Pei, S., & Cheng, H. M. (2012). The reduction of graphene oxide. *Carbon*, 50(9), 3210-3228. <https://doi.org/10.1016/j.carbon.2011.11.010>
- Pitchaipillai, R., & Ponniah, T. (2016). In vitro antidiabetic activity of ethanolic leaf extract of bruguiera *Cylindrica* L.–glucose uptake by yeast cells method. *International Biological and Biomedical Journal*, 2(4), 171-175. <https://ibbj.org/article-1-92-en.pdf>
- Potbhare, A. K., Aziz, S. T., Ayyub, M. M., Kahate, A., Madankar, R., Wankar, S., ... & Chaudhary, R. G. (2024). Bioinspired graphene-based metal oxide nanocomposites for photocatalytic and electrochemical performances: an updated review. *Nanoscale Advances*, 6(10), 2539-2568. <https://doi.org/10.1039/d3na01071f>
- Rajapaksha, P., Orrell-Trigg, R., Shah, D., Cheeseman, S., Vu, K. B., Ngo, S. T., ... & Chapman, J. (2023). Broad spectrum antibacterial zinc oxide-reduced graphene oxide nanocomposite for water depollution. *Materials Today Chemistry*, 27, 101242. <https://doi.org/10.1016/j.mtchem.2022.101242>

- Ramesh, S., Vinitha, U. G., Anthony, S. P., & Muthuraman, M. S. (2021). Pods of *Acacia nilotica* mediated synthesis of copper oxide nanoparticles and its in vitro biological applications. *Materials Today: Proceedings*, 47, 751-756. <https://doi.org/10.1016/j.matpr.2020.07.052>
- Saravanan, H., Subramani, T., Rajaramon, S., David, H., Sajeevan, A., Sujith, S., & Solomon, A. P. (2023). Exploring nanocomposites for controlling infectious microorganisms: Charting the path forward in antimicrobial strategies. *Frontiers in Pharmacology*, 14, 1282073. <https://doi.org/10.3389/fphar.2023.1282073>
- Sharma, B. K., Saha, A., Rahaman, L., Bhattacharjee, S., & Tribedi, P. (2015). Silver inhibits the biofilm formation of *Pseudomonas aeruginosa*. *Advances in Microbiology*, 5(10), 677-685. <https://doi.org/10.4236/aim.2015.510070>
- Sharma, P., Kumar, N., Chauhan, R., Singh, V., Srivastava, V. C., & Bhatnagar, R. (2020). Growth of hierarchical ZnO nano flower on large functionalized rGO sheet for superior photocatalytic mineralization of antibiotic. *Chemical Engineering Journal*, 392, 123746. <https://doi.org/10.1016/j.cej.2019.123746>
- Sirelkhatim, A., Mahmud, S., Seeni, A., Kaus, N. H. M., Ann, L. C., Bakhori, S. K. M., ... & Mohamad, D. (2015). Review on zinc oxide nanoparticles: antibacterial activity and toxicity mechanism. *Nano-micro-Letters*, 7(3), 219-242. <https://doi.org/10.1007/s40820-015-0040-x>
- Slowing, I. I., Wu, C. W., Vivero-Escoto, J. L., & Lin, V. S. Y. (2009). Mesoporous silica nanoparticles for reducing hemolytic activity towards mammalian red blood cells. *Small*, 5(1), 57-62. <https://doi.org/10.1002/smll.200800926>
- Sodeinde, K. O., Olusanya, S. O., Lawal, O. S., Sriariyanun, M., & Adediran, A. A. (2022). Enhanced adsorptional-photocatalytic degradation of chloramphenicol by reduced graphene oxide-zinc oxide nanocomposite. *Scientific Reports*, 12(1), 17054. <https://doi.org/10.1038/s41598-022-21266-5>
- Sportelli, M. C., Gaudiuso, C., Volpe, A., Izzì, M., Picca, R. A., Ancona, A., & Cioffi, N. (2022). Biogenic synthesis of ZnO nanoparticles and their application as bioactive agents: a critical overview. *Reactions*, 3(3), 423-441. <https://doi.org/10.3390/reactions3030030>
- Sruthi, S., Ashtami, J., & Mohanan, P. V. (2018). Biomedical application and hidden toxicity of Zinc oxide nanoparticles. *Materials Today Chemistry*, 10, 175-186. <https://doi.org/10.1016/j.mtchem.2018.09.008>
- Stefanidou, M., Maravelias, C., Dona, A., & Spiliopoulou, C. (2006). Zinc: A multipurpose trace element. *Archives of toxicology*, 80(1), 1-9. <https://doi.org/10.1007/s00204-005-0009-5>
- Sun, M., Liu, H., Liu, Y., Qu, J., & Li, J. (2015). Graphene-based transition metal oxide nanocomposites for the oxygen reduction reaction. *Nanoscale*, 7(4), 1250-1269. <https://doi.org/10.1039/c4nr05838k>
- Tai, H., Yuan, Z., Zheng, W., Ye, Z., Liu, C., & Du, X. (2016). ZnO nanoparticles/reduced graphene oxide bilayer thin films for improved NH<sub>3</sub>-sensing performances at room temperature. *Nanoscale Research Letters*, 11(1), 130. <https://doi.org/10.1186/s11671-016-1343-7>
- Wahba, N. S., Shaban, S. F., Kattaia, A. A., & Kandeel, S. A. (2016). Efficacy of zinc oxide nanoparticles in attenuating pancreatic damage in a rat model of streptozotocin-induced diabetes. *Ultrastructural Pathology*, 40(6), 358-373. <https://doi.org/10.1080/01913123.2016.1246499>
- Wiesmann, N., Tremel, W., & Brieger, J. (2020). Zinc oxide nanoparticles for therapeutic purposes in cancer medicine. *Journal of Materials Chemistry B*, 8(23), 4973-4989. <https://doi.org/10.1039/d0tb00739k>
- Yadav, N., & Lochab, B. (2019). A comparative study of graphene oxide: Hummers, intermediate and improved method. *FlatChem*, 13, 40-49. <https://doi.org/10.1016/j.flatc.2019.02.001>
- Yang, K., Feng, L., Shi, X., & Liu, Z. (2013). Nano-graphene in biomedicine: theranostic applications. *Chemical Society Reviews*, 42(2), 530-547. <https://doi.org/10.1039/c2cs35342c>
- Yu, H., Zhang, B., Bulin, C., Li, R., & Xing, R. (2016). High-efficient synthesis of graphene oxide based on improved hummers method. *Scientific Reports*, 6(1), 36143. <https://doi.org/10.1038/srep36143>
- Yuvakkumar, R., Suresh, J., Nathanael, A. J., Sundrarajan, M., & Hong, S. I. (2014). Novel green synthetic strategy to prepare ZnO nanocrystals using rambutan (*Nephelium lappaceum* L.) peel extract and its antibacterial applications. *Materials Science and Engineering: C*, 41, 17-27. <https://doi.org/10.1016/j.msec.2014.04.025>
- Zhang, X., Wei, W., Wang, K., Xiao, G., & Xu, M. (2020). Graphene reinforced carbon nanofiber engineering enhances Li storage performances of germanium oxide. *RSC advances*, 10(18), 10873-10878. <https://doi.org/10.1039/D0RA00720J>